

NANO EXPRESS

Open Access

SiO_x/SiN_y multilayers for photovoltaic and photonic applications

Ramesh Pratibha Nalini^{1*}, Larysa Khomenkova¹, Olivier Debieu¹, Julien Cardin¹, Christian Dufour¹, Marzia Carrada² and Fabrice Gourbilleau¹

Abstract

Microstructural, electrical, and optical properties of undoped and Nd³⁺-doped SiO_x/SiN_y multilayers fabricated by reactive radio frequency magnetron co-sputtering have been investigated with regard to thermal treatment. This letter demonstrates the advantages of using SiN_y as the alternating sublayer instead of SiO₂. A high density of silicon nanoclusters of the order 10¹⁹ nc/cm³ is achieved in the SiO_x sublayers. Enhanced conductivity, emission, and absorption are attained at low thermal budget, which are promising for photovoltaic applications. Furthermore, the enhancement of Nd³⁺ emission in these multilayers in comparison with the SiO_x/SiO₂ counterparts offers promising future photonic applications.

PACS: 88.40.fh (Advanced materials development), 81.15.cd (Deposition by sputtering), 78.67.bf (Nanocrystals, nanoparticles, and nanoclusters).

Keywords: SiO_x/SiN_y, multilayers, Nd³⁺ doping, photoluminescence, XRD, absorption coefficient, conductivity

Introduction

Silicon nanoclusters [Si-ncs] with engineered band gap [1] have attracted the photonic and the photovoltaic industries as potential light sources, optical interconnectors, and efficient light absorbers [2-5]. Multilayers [MLs] of silicon-rich silicon oxide [SiO_x] alternated with SiO₂ became increasingly popular due to the precise control on the density and size distribution of Si-ncs [6,7]. Moreover, the efficiency of light emission from SiO_x-based MLs exceeds that of the single SiO_x layers with equivalent thickness due to the narrower Si-nc size distribution. The ML approach is also a powerful tool to investigate and control the emission of rare-earth [RE] dopants, for example, Er-doped SiO_x/SiO₂ MLs [8]. It also allows us to control the excitation mechanism of the RE ions by adjusting the optimal interaction distance between the Si-ncs and the RE ions. However, achieving electroluminescence and hence extending its usage for photovoltaic applications are problematic due to the high resistivity caused by SiO₂ barrier layers [9]. Hence, replacement of the SiO₂ sublayer by alternative

dielectrics becomes interesting. Due to the lower potential barrier and better electrical transport properties of silicon nitride [Si₃N₄] in comparison to SiO₂, multilayers like SiO_x/Si₃N₄ [10], Si-rich Si₃N₄ (SiN_y)/Si₃N₄ [11], and Si-rich Si₃N₄/SiO₂ [12] were proposed and investigated [13] for their optical and electrical properties.

In this letter, we investigate SiO_x/SiN_y MLs and compare them with the SiO_x/SiO₂ counterparts reported earlier [9,14]. We demonstrate that an enhancement in the conductive and light-emitting properties of SiO_x/SiN_y MLs can be achieved with a reduced thermal budget. We also report a pioneering study on Nd-doped SiO_x/SiN_y MLs. A comparison between the properties of Nd³⁺-doped SiO_x/SiO₂ and SiO_x/SiN_y MLs are presented, and we show the benefits of using SiN_y sublayers to achieve enhanced emission from Nd³⁺ ions.

Experimental details

Undoped and Nd-doped 3.5-nm SiO_x/5-nm SiN_y (50 periods) MLs were deposited at 500°C on a 2-inch p-Si substrate by radio frequency [RF] magnetron co-sputtering of Si and SiO₂ targets in hydrogen-rich plasma for the SiO_x sublayers and a pure Si target in nitrogen-rich plasma for the SiN_y sublayers. An additional Nd₂O₃ target was used to dope the SiO_x and SiN_y sublayers by

* Correspondence: pratibha-nalini.sundar@ensicaen.fr

¹CIMAP UMR CNRS/CEA/ENSICAEN/UCBN, 6 Bd. Maréchal Juin, 14050 Caen Cedex 4, France

Full list of author information is available at the end of the article

Nd^{3+} ions. More details on the growth process can be found elsewhere [15]. The excess Si content in the corresponding SiO_x and SiN_y single layers obtained from RBS studies are calculated to be 25 and 11 at.%, respectively (i.e., $\text{SiO}_{x=1}$ and $\text{SiN}_{y=1.03}$). Conventional furnace annealing under nitrogen atmosphere at different temperatures, $T_A = 400$ to $1,100^\circ\text{C}$, and times, $t_A = 1$ to 60 min, was performed on the MLs. X-ray diffraction analysis was performed using a Phillips XPERT HPD Pro device (PANalytical, Almelo, The Netherlands) with CuK_α radiation ($\lambda = 0.1514$ nm) at a fixed grazing angle incidence of 0.5° . Asymmetric grazing geometry was chosen to increase the volume of material interacting with the X-ray beam and to eliminate the contribution of the Si substrate. Photoluminescence [PL] spectra were recorded in the 550- to 1,150-nm spectral range using the Triax 180 Jobin Yvon monochromator (HORIBA Jobin Yvon SAS, Longjumeau, Paris, France) with an R5108 Hamamatsu PM tube (Hamamatsu, Shizuoka, Japan). The 488-nm Ar^+ laser line served as the excitation source. All the PL spectra were corrected by the spectral response of the experimental setup. Top and rear-side gold contacts were deposited on the MLs by sputtering for electrical characterization. Current-voltage measurements were carried out using a SUSS Microtec EP4 two-probe apparatus (SUSS Microtec, Germany) equipped with Keithley devices (Keithly, Cleveland, OH, USA). Energy-filtered transmission electron microscopy [EFTEM] was carried out on a cross-sectional specimen using a TEM-FEG microscope Tecnai F20ST (FEI, Eindhoven, The Netherlands) equipped with an energy filter TRIDIEM from Gatan (Gatan, München, Germany). The EFTEM images were obtained by inserting an energy-selecting slit in the energy-dispersive plane of the filter at the Si (17 eV) and at the SiO_2 (23 eV) plasmon energy, with a width of ± 2 eV.

Results and discussions

Effect of annealing on the PL

Since an annealing at $T_A = 1,100^\circ\text{C}$ and $t_A = 60$ min is the most suitable to achieve an efficient PL from Si-ncs either in sputtered SiO_x single layers [7] or in $\text{SiO}_x/\text{SiO}_2$ MLs [16], such treatment was first employed on $\text{SiO}_x/\text{SiN}_y$ MLs. The X-ray diffraction [XRD] broad peak centered around $2\theta = 28^\circ$ is the signature of the Si nanoclusters' formation in the $\text{SiO}_x/\text{SiO}_2$ (Figure 1, curve 1) and $\text{SiO}_x/\text{SiN}_y$ MLs (Figure 1, curve 2) as already observed by means of atomic scale studies on similar multilayers [17]. However, contrary to the PL emission obtained from the $\text{SiO}_x/\text{SiO}_2$ MLs, no PL emission was observed in the $\text{SiO}_x/\text{SiN}_y$ MLs after such annealing (Figure 2a). This stimulated a deeper investigation of the post-fabrication processing to achieve efficient light emission from the $\text{SiO}_x/\text{SiN}_y$ MLs.

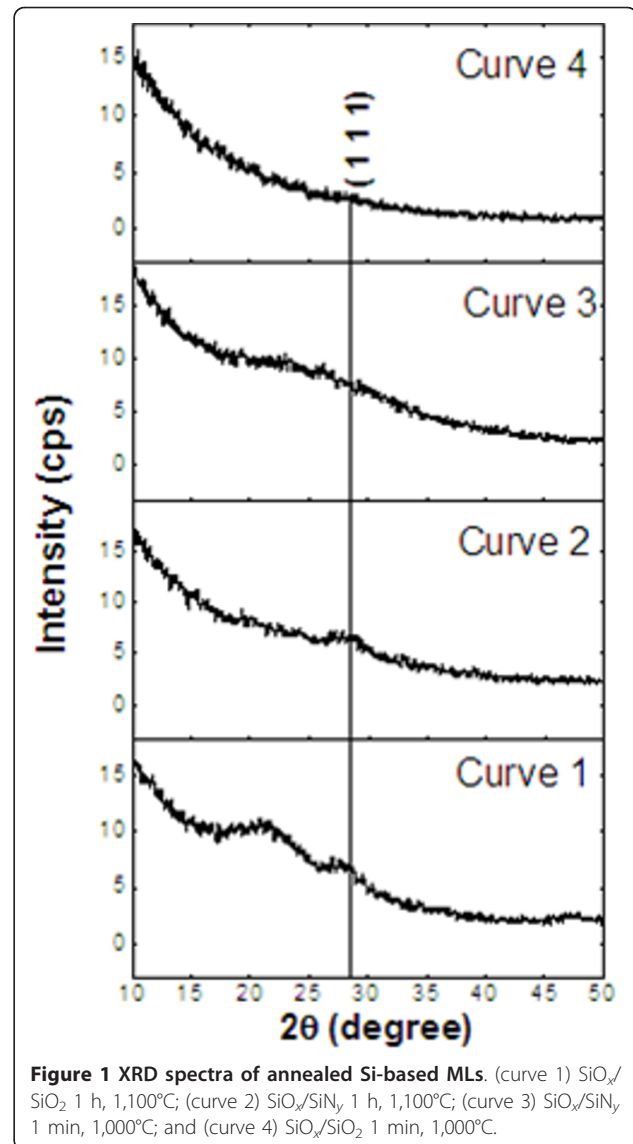
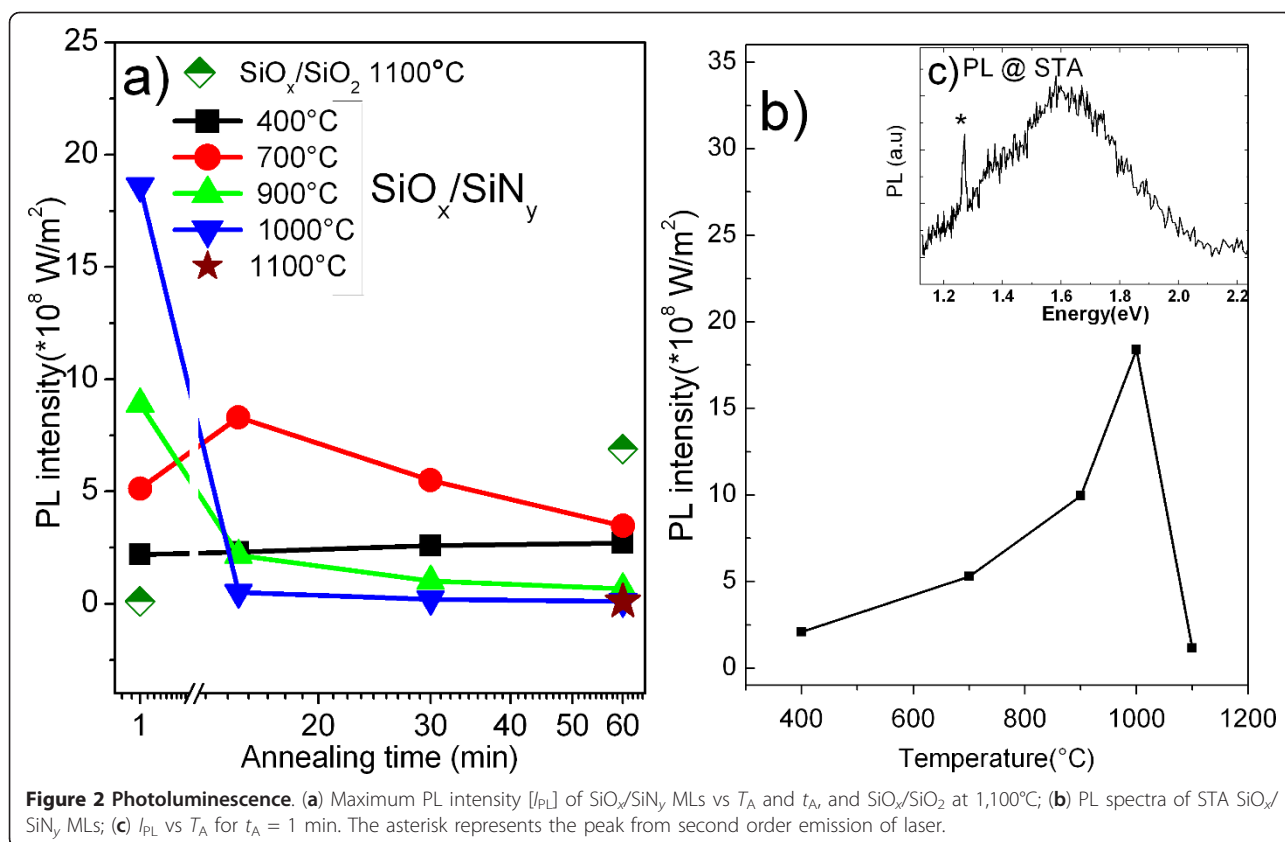


Figure 1 XRD spectra of annealed Si-based MLs. (curve 1) $\text{SiO}_x/\text{SiO}_2$ 1 h, $1,100^\circ\text{C}$; (curve 2) $\text{SiO}_x/\text{SiN}_y$ 1 h, $1,100^\circ\text{C}$; (curve 3) $\text{SiO}_x/\text{SiN}_y$ 1 min, $1,000^\circ\text{C}$; and (curve 4) $\text{SiO}_x/\text{SiO}_2$ 1 min, $1,000^\circ\text{C}$.

It was observed that the PL signals from the MLs annealed during $t_A = 60$ min are significant only at lower temperatures ($T_A = 400^\circ\text{C}$ to 700°C), and high intensities are obtained when the samples are annealed at high temperatures for a short time ($T_A = 900^\circ\text{C}$ to $1,000^\circ\text{C}$, $t_A = 1$ min). It is interesting to note that an interplay between T_A and t_A can yield similar PL efficiencies, as can be seen for $T_A = 900^\circ\text{C}$ and $t_A = 1$ min, and $T_A = 700^\circ\text{C}$ and $t_A = 15$ min (Figure 2a).

The highest PL intensity in $\text{SiO}_x/\text{SiN}_y$ MLs was obtained with $T_A = 1,000^\circ\text{C}$ and $t_A = 1$ min (Figure 2b, c), whereas the $\text{SiO}_x/\text{SiO}_2$ MLs showed no emission after such short-time annealing treatment (Figure 2a). Corresponding XRD pattern of this short-time annealed [STA] (STA = 1 min, $1,000^\circ\text{C}$) $\text{SiO}_x/\text{SiN}_y$ showed a broad peak in the range $2\theta = 20^\circ$ to 30° which is absent



in STA $\text{SiO}_x/\text{SiO}_2$ MLs (Figure 1, curves 3 and 4). This suggests the presence of small Si clusters in the $\text{SiO}_x/\text{SiN}_y$ MLs, with lower sizes (broader peak) by comparison with higher annealing temperature (1,100°C; Figure 1, curves 1 and 2). However, we cannot distinguish which of the sublayer is at the origin of the PL emission. Consequently, the recorded PL may be a combined contribution of the Si-ncs in the SiO_x sublayers and the localized bandtail defect states in the SiN_y sublayers.

Absorption and electrical studies

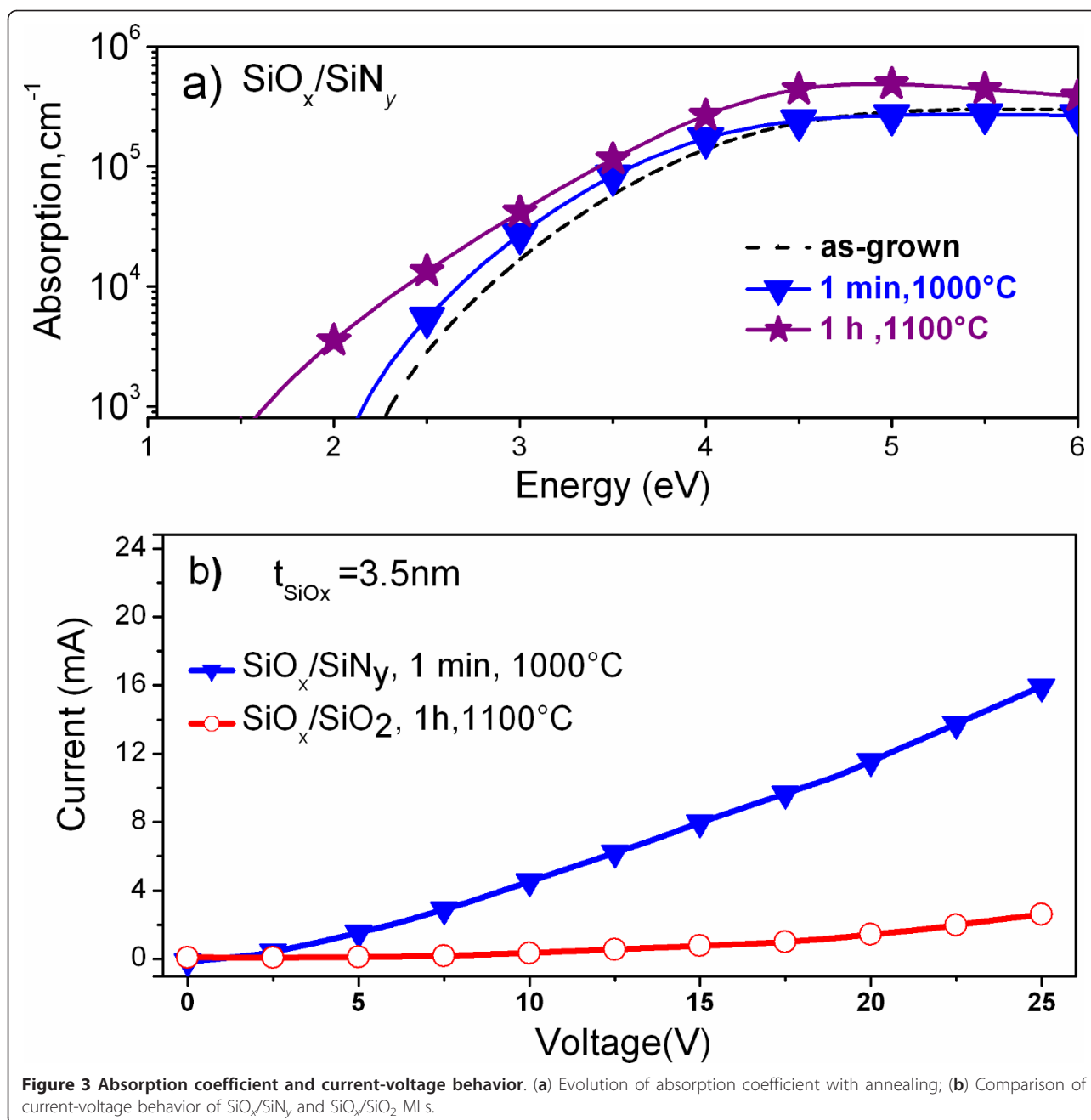
The absorption studies show similar absorption coefficients for as-grown and STA MLs, whereas annealing at $T_A = 1,100^\circ\text{C}$ and $t_A = 60$ min results in an absorption enhancement (Figure 3a). One can say that, at such temperature, an increase in density and size of the Si-ncs occurs due to phase separation of the SiO_x sublayers into Si and SiO_2 phases. The formation of Si nanocrystals is complete at $T_A = 1,100^\circ\text{C}$ and $t_A = 60$ min and leads to this enhancement. This reasoning is supported by the results obtained from the PL and the XRD analysis of the samples annealed at such temperature. The PL in the $\text{SiO}_x/\text{SiN}_y$ MLs is quenched after an increase in the time and temperatures of annealing (Figure 2a), and this can be attributed to the increase in the size leading to the loss of quantum confinement effect. The

formation of Si nanoclusters can be witnessed from the appearance of the XRD peak at $2\theta = 28^\circ$ (Figure 1, curve 2), which is not seen in the short-time annealed sample (Figure 1, curve 3).

Considering a balance between light emission and absorption for photovoltaic applications, we chose to study STA $\text{SiO}_x/\text{SiN}_y$ MLs with a total thickness of 850 nm for electrical measurements. Figure 3b compares the dark current curves of 3.5-nm $\text{SiO}_x/5$ -nm SiN_y , with our earlier reported 3.5-nm $\text{SiO}_x/3.5$ -nm SiO_2 (140 nm) MLs [14]. The resistivity was calculated at 7.5 V to be 2.15 and 214 $\text{M}\Omega\cdot\text{cm}$ in the $\text{SiO}_x/\text{SiN}_y$ and $\text{SiO}_x/\text{SiO}_2$ MLs, respectively. Since the thickness of the SiO_x sublayer is the same in both cases (3.5 nm), this decrease in the resistivity of the $\text{SiO}_x/\text{SiN}_y$ MLs can be ascribed to the substitution of 3.5-nm SiO_2 by 5-nm SiN_y sublayers. This hundred-times enhanced conductivity at low voltage paves way for further improvement of the $\text{SiO}_x/\text{SiN}_y$ MLs' conductivity, for example, by decreasing the thickness of this SiN_y sublayer.

Microstructural studies

The high-resolution transmission electron microscope [HRTEM] and EFTEM observations on STA $\text{SiO}_x/\text{SiN}_y$ show Si-ncs in the SiO_x sublayers with an average diameter of 3.4 nm. Only a couple of Si nanocrystals were

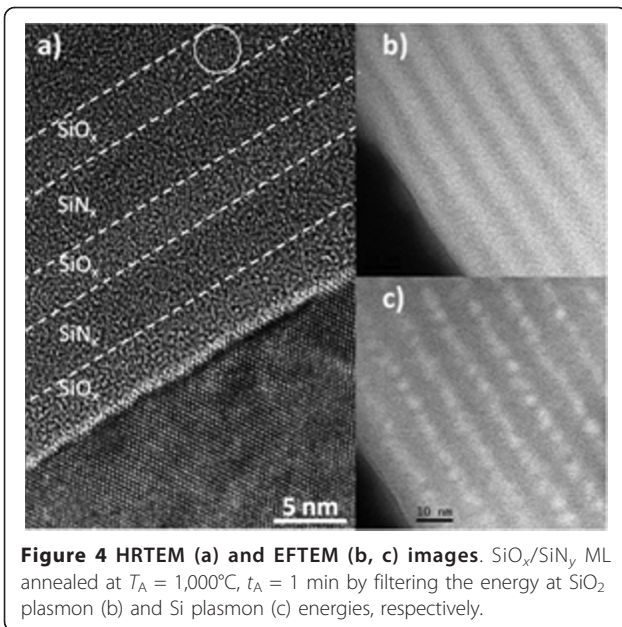


observed in the HRTEM (Figure 4a), whereas a high density of Si-nanoclusters of about 10^{19} nc/cm^3 can be witnessed from the EFTEM images taken at the Si plasmon energy (Figure 4c) implying that they are predominantly amorphous. Interestingly, this density of the Si-ncs in the $\text{SiO}_x/\text{SiN}_y$ MLs is an order of magnitude higher than the Si-ncs formed in the $\text{SiO}_x/\text{SiO}_2$ MLs fabricated under similar conditions. The brighter SiO_x sublayers are distinguished from the darker SiN_y sublayers by filtering the SiO_2 plasmon energy (Figure 4b). No evidence of Si-ncs within the SiN_x sublayers was

obtained. The STA could favor the formation of Si-ncs only in SiO_x and not in SiN_y sublayers. This could be attributed to the different mechanism of Si-ncs formation in SiO_x and SiN_y in MLs as opposed to that in single layers [18] and/or the low Si-excess content in SiN_y .

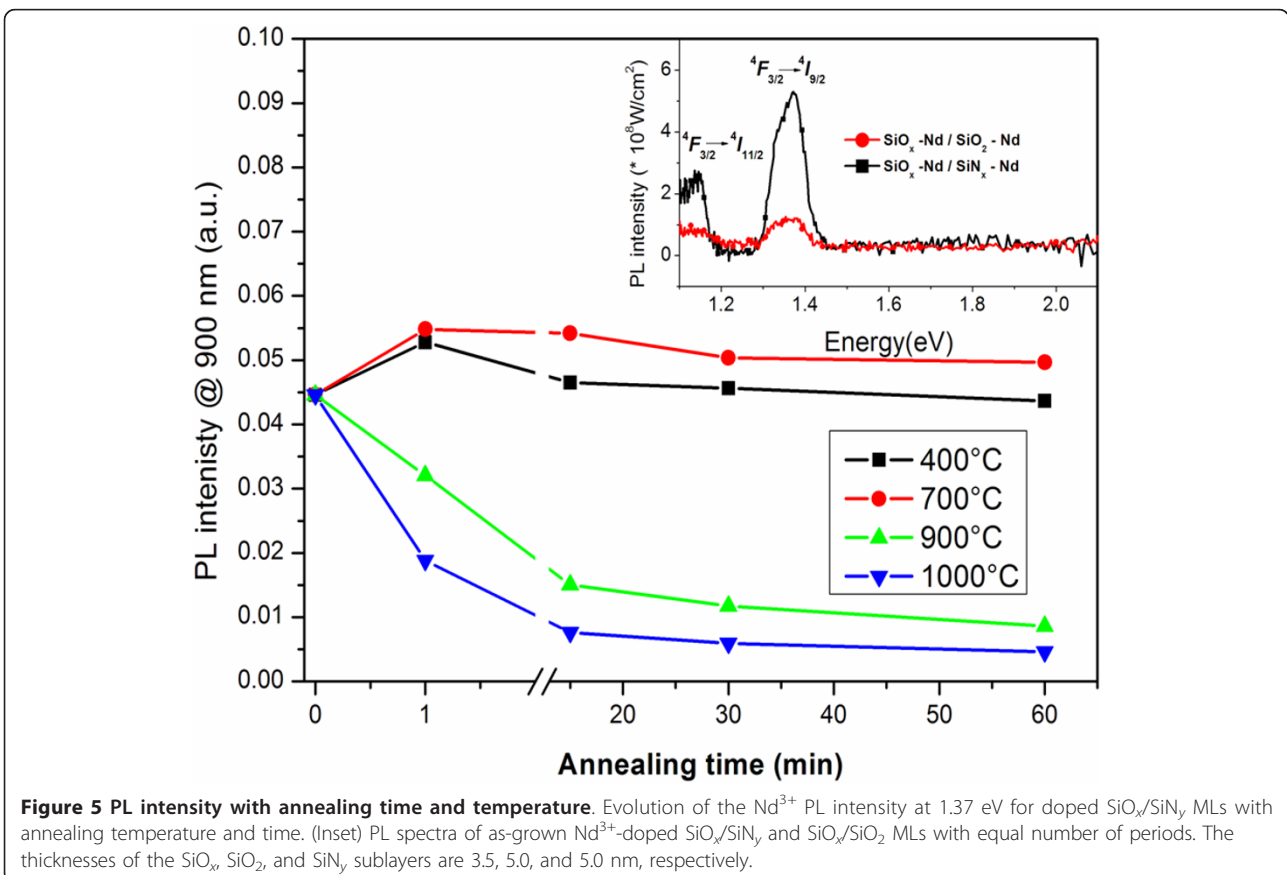
Effect of Nd^{3+} -doping

Understanding the microstructure of MLs and considering the enhancement of absorption and emission properties in $\text{SiO}_x/\text{SiN}_y$ MLs compared to the $\text{SiO}_x/\text{SiO}_2$ MLs, we investigate the effect of using SiN_y sublayer on



the PL emission from Nd^{3+} ions. For this purpose, the $\text{SiO}_x\text{-Nd}/\text{SiN}_y\text{-Nd}$ and $\text{SiO}_x\text{-Nd}/\text{SiO}_2\text{-Nd}$ MLs were fabricated, and their PL properties were compared. No PL emission was detected from the Nd^{3+} -doped SiN_y single

layers at the different annealing treatments investigated here. Figure 5 shows the PL spectra of the Nd^{3+} -doped as-grown MLs under non-resonant excitation with peaks corresponding to the ${}^4F_{3/2} \rightarrow {}^4I_{9/2}$ and ${}^4F_{3/2} \rightarrow {}^4I_{11/2}$ transitions at 1.37 and 1.17 eV, respectively. The comparison between the PL properties of undoped (Figure 2c) and Nd^{3+} -doped MLs (Figure 5, inset) clearly shows the quenching of visible PL emission and the appearance of two Nd^{3+} -related PL peaks in the Nd -doped MLs. Moreover, the intensity of Nd^{3+} PL from the doped $\text{SiO}_x/\text{SiN}_y$ MLs exceeds that of the $\text{SiO}_x/\text{SiO}_2$ MLs (Figure 5, inset). Thus, we deal with the efficient energy transfer towards Nd^{3+} ions not only in SiO_x but also in SiN_y sublayers. Since this emission is observed for as-grown MLs, when no Si-ncs were formed in these MLs, it is obvious that the emission from the Nd^{3+} ions in the $\text{SiN}_x\text{-Nd}$ sublayers is due to an efficient energy transfer from SiN_y -localized defect states towards the Nd^{3+} ions [19,20]. PL observed from the doped MLs after STA was not intense, and it was quenched with increasing annealing time. The same behavior was observed for the 900°C annealing. This could be due to the decrease in the number of defect-related sensitizers in SiN_y and the formation of Nd_2O_3 clusters in the SiO_x sublayers [21]. On the other hand, annealing at $T_A = 400^\circ\text{C}$ to 700°C ,



discussed above for the undoped $\text{SiO}_x/\text{SiN}_y$ MLs, enhance Nd^{3+} PL emission when applied to the doped counterparts (Figure 3). Thus, we attain intense PL at a low thermal budget with T_A (400°C to 700°C) and t_A (1 min). To optimize Nd^{3+} emission, the effect of the thickness of each sublayer in $\text{SiO}_x/\text{SiN}_y$ MLs is under consideration now.

Conclusion

In conclusion, we show that $\text{SiO}_x/\text{SiN}_y$ MLs fabricated by RF magnetron sputtering can be engineered as structures for photovoltaic and photonic applications. The as-grown and STA $\text{SiO}_x/\text{SiN}_y$ MLs show enhanced optical and electrical properties than the $\text{SiO}_x/\text{SiO}_2$ counterparts. Besides achieving a high density of Si-ncs at a reduced thermal budget, we show that high emission and absorption efficiencies can be achieved even from amorphous Si-ncs. The Nd-doped MLs, as-grown and those annealed at lower thermal budgets, demonstrate efficient emission from rare-earth ions. We also show that our STA $\text{SiO}_x/\text{SiN}_y$ MLs have about a hundred times higher conductivity compared to the $\text{SiO}_x/\text{SiO}_2$ MLs. These results show the advantages of $\text{SiO}_x/\text{SiN}_y$ MLs as materials for photovoltaic and photonic applications and open up perspectives for a detailed study.

Abbreviations

MLs: multilayers; PL: photoluminescence; Si-nc: silicon nanoclusters; SiN_y : silicon-rich silicon nitride; SiO_x : silicon-rich silicon oxide; STA: short time annealing at 1,000°C for 1 min.

Acknowledgements

This study is supported by the DGA (Defense Procurement Agency) through the research program no. 2008.34.0031. The authors acknowledge J. Pierrière for the RBS measurements done with the SAFIR accelerator (INSP, UPMC) and X. Portier (CIMAP) for the TEM image.

Author details

¹CIMAP UMR CNRS/CEA/ENSICAEN/UCBN, 6 Bd. Maréchal Juin, 14050 Caen Cedex 4, France ²CEMES/CNRS, 29 rue J. Marvig, 31055 Toulouse, France

Authors' contributions

RPN fabricated the undoped multilayers under investigation and carried out the characterization studies. LK and OD fabricated the Nd-doped layers and studied the effect of Nd doping on the MLs. JC and CD made contributions to the optical studies. MC performed the EFTM measurements. FG conceived of the study and participated in the coordination of the manuscript. All authors read and approved the final manuscript.

Competing interests

The authors declare that they have no competing interests.

Received: 11 October 2011 Accepted: 14 February 2012

Published: 14 February 2012

References

1. Canham LT: Silicon quantum wire array fabrication by electrochemical and chemical dissolution of wafers. *Appl Phys Lett* 1990, **57**:1046.
2. Pavesi L, Dal Negro L, Mazzoleni C, Franzo G, Priolo F: Optical gain in silicon nanocrystals. *Nature* 2000, **408**:440.

3. Irrera A, Franzo G, Iacona F, Canino A, Di Stefano G, Sanfilippo D, Piana A, Fallica PG, Priolo F: Light emitting devices based on silicon nanostructures. *Physica E* 2007, **38**:181.
4. Garrido B, Lopez M, Pérez Rodriguez A, Garcia C, Pellegrino P, Ferré R, Moreno JA, Morante JR, Bonafas C, Carrada M, Claverie A, De La Torre J, Souifi A: Optical and electrical properties of silicon nanocrystals ion-beam synthesized in SiO_2 . *Nucl Inst Meth Phys B* 2004, **216**:231.
5. Conibeer G, Green MA, Corkish R, Cho Y, Cho EC, Jiang CW, Fangsuwannarak T, Pink E, Huang Y, Puzzer T, Trupke T, Richards B, Shalav A, Lin KL: Silicon nanostructures for third generation photovoltaic solar cells. *Thin Solid Films* 2006, **511**:654.
6. Zacharias M, Heitmann J, Scholz R, Kahler U, Schimdt M, Blasing J: Size controlled highly luminescent silicon nanocrystals: a SiO/SiO_2 superlattice approach. *Appl Phys Lett* 2002, **80**:661.
7. Gourbilleau F, Portier X, Ternon C, Voivenel V, Madelon R, Rizk R: Si-rich/ SiO_2 nanostructured multilayers by reactive magnetron sputtering. *Appl Phys Lett* 2001, **78**:3058.
8. Gourbilleau F, Dufour C, Madelon R, Rizk R: Effects of Si nanocluster size and carrier Er interaction distance on the efficiency of energy transfer. *J Lumin* 2007, **126**:581.
9. Maestre D, Palais O, Barakel D, Pasquinelli M, Alfonso C, Gourbilleau F, De Laurentis M, Irace A: Structural and optoelectronic characterization of Si- $\text{SiO}_2/\text{SiO}_2$ multilayers with applications in all Si tandem solar cells. *J Appl Phys* 2010, **107**:064321.
10. Di D, Perez-Wurfl I, Conibeer G, Green MA: Formation and photoluminescence of Si quantum dots in $\text{SiO}_2/\text{Si}_3\text{N}_4$ hybrid matrix for all-Si tandem solar cells. *Solar Energy Materials & Solar Cells* 2010, **94**:2238.
11. So YH, Huang S, Conibeer G, Green MA: Formation and photoluminescence of Si nanocrystals in controlled multilayer structure comprising of Si-rich nitride and ultrathin silicon nitride barrier layers. *Thin Solid Films* 2011, **519**:5408.
12. Delachat F, Carrada M, Ferblantier G, Grob JJ, Slaoui A, Rinnert H: The structural and optical properties of SiO_2/Si rich SiN_x multilayers containing Si-ncs. *Nanotechnology* 2009, **20**:275608.
13. Conibeer G, Green MA, Perez-Wurfl I, Huang S, Hao X, Di D, Shi L, Shrestha S, Puthen-Veetil B, So Y, Zhang B, Wan Z: Silicon quantum dot based solar cells: addressing the issues of doping, voltage and current transport. *Prog Photovolt: Res Appl* Paper presented at the 25th EU PVSEC WCPEC-5, Spain; 2010.
14. Pratibha Nalini R, Dufour C, Cardin J, Gourbilleau F: New Si-based multilayers for solar cell applications. *Nanoscale Res Lett* 2011, **6**:156.
15. Ternon C, Gourbilleau F, Portier X, Voivenel P, Dufour C: An original approach for the fabrication of Si/ SiO_2 multilayers using reactive magnetron sputtering. *Thin Solid Films* 2002, **419**:5.
16. Gourbilleau F, Ternon C, Maestre D, Palais O, Dufour C: Silicon-rich $\text{SiO}_2/\text{SiO}_2$ multilayers: a promising material for the third generation of solar cell. *J Appl Phys* 2009, **106**:013501.
17. Talbot E, Lardé M, Gourbilleau F, Dufour C, Pareige P: Si nanoparticles in SiO_2 : an atomic scale observation for optimization of optical devices. *EPL* 2009, **87**:26004.
18. Dal Negro L, Yi JH, Michel J, Kimerling MC, Chang TWF, Sukhovatkin V, Sargent EH: Light emission efficiency and dynamics in silicon-rich silicon nitride films. *Appl Phys Lett* 2006, **88**:233109.
19. Biggemann D, Tessler LR: Near infra-red photoluminescence of Nd^{3+} in hydrogenated amorphous silicon sub-nitrides a- SiN_xH <Nd>. *Mat Sci Eng B* 2003, **105**:188.
20. Lin R, Yerci S, Kucheyev SO, Van Buuren T, Dal Negro L: Energy transfer and stimulated emission dynamics at 1.1 μm in Nd-doped SiN_x . *Optics Express* 2011, **19**:5379.
21. Debieu O, Bréard D, Podhorodecki A, Zatyry G, Misiewicz J, Labbé C, Cardin J, Gourbilleau F: Effect of annealing and Nd concentration on the photoluminescence of Nd^{3+} ions coupled with silicon nanoparticles. *J Appl Phys* 2010, **108**:113114.

doi:10.1186/1556-276X-7-124

Cite this article as: Nalini et al.: $\text{SiO}_x/\text{SiN}_y$ multilayers for photovoltaic and photonic applications. *Nanoscale Research Letters* 2012 **7**:124.